



Characterization and single cell testing of Pt/C electrodes prepared by electrodeposition[☆]

A.J. Martín^a, A.M. Chaparro^{a,*}, B. Gallardo^a, M.A. Folgado^a, L. Daza^{a,b}

^a CIEMAT, Department of Energy, Avda. Complutense 22, 28040 Madrid, Spain

^b Instituto de Catálisis y Petroleoquímica (CSIC), C/. Marie Curie 2, Campus Cantoblanco, 28049 Madrid, Spain

ARTICLE INFO

Article history:

Received 10 October 2008

Accepted 24 October 2008

Available online 6 November 2008

Keywords:

PEMFC
Electrodeposition
Porous electrode
Platinum
Fuel cell

ABSTRACT

Electrodes for proton exchange membrane fuel cells (PEMFC) have been prepared by the electrodeposition method. For this task, the electrodeposition of platinum is carried out on a carbon black substrate impregnated with an ionomer, proton conducting, medium. Before electrodeposition, the substrate is submitted to an activation process to increase the hydrophilic character of the surface to a few microns depth.

Electrodeposition of platinum takes place inside the generated surface hydrophilic layer, resulting in a continuous phase covering totally or partially carbon substrate grains. Cross sectional images show a decay profile of platinum towards the interior of the substrate, reflecting a deposition process limited by diffusion of PtCl_6^{2-} through the porous substrate. Electrodes with different platinum loads have been prepared, and membrane electrode assemblies (MEA) have been mounted with the electrodeposited electrodes as cathode and other standard components (commercial anode and Nafion[®] 117 membrane). The electrochemically active surface area determined from hydrogen underpotential deposition charge, is lower on the electrodeposited electrodes than on standard electrodes. However, single cell testing shows higher mass specific activity on electrodeposited cathodes with low and intermediate Pt load (below $0.05 \text{ mg Pt cm}^{-2}$).

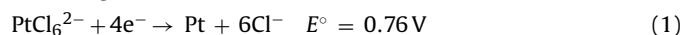
© 2008 Elsevier B.V. All rights reserved.

1. Introduction

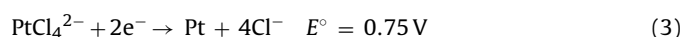
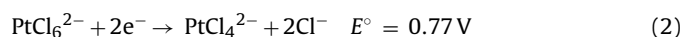
Most challenges related with proton exchange membrane fuel cells (PEMFC) reside in the electrodes, including the improvement of efficiency, life time, and cost. For this reason, the synthesis of the electrocatalyst and electrode fabrication, have become matters of basic and applied research for many groups. One technique of interest for PEMFC electrode fabrication is based on the electrodeposition of platinum [1–8]. The electrodeposition of platinum is a process used for different industrial applications, like fabrication of aviation components, electrodes, turbine blades, and in jewellery [1]. When applied for PEMFC gas diffusion electrodes, electrocatalyst synthesis and electrode fabrication take place at once, because platinum particles can be synthesised and deposited on the gas diffusion layer (carbon black substrate). Electrodeposition for PEMFC electrode fabrication has been carried out following different procedures. Platinum precursor impregnation with active layer components, carbon black and ionomer, before electroreduction, improves the interaction with carbon surface grains to

allow for high catalyst loads [2,3]. ‘Through-membrane’ deposition has also been used, using positively charged platinum precursors able to cross a thick cationic exchange membrane [4,5]. Direct deposition from aqueous solution on the carbon black substrate, previously submitted to a wetting procedure, has been carried out by means of current pulse electrodeposition, giving rise to Pt particles located in a thin layer, and demonstrating good performance as PEMFC electrode [6,7]. When compared with standard electrodes, electrodeposited electrodes show higher mass activities [8].

Different electrolyte compositions may be used, both in basic or acidic solutions, for platinum electrodeposition [9]. Hexachloroplatinic acid (H_2PtCl_6), a compound resulting from the refining of platinum concentrates by solvent extraction, is the most common precursor due to its availability, stability, and good solubility in acid media [10]. This compound reduces to metallic platinum according to:



Reaction (1) appears to be mediated by formation of PtCl_4^{2-} [11]:



If reaction (3) is slower than reaction (2), part of the intermediate PtCl_4^{2-} may remain in solution resulting in a decrease in

[☆] Presented at CONAPPICE 2008, Zaragoza, Spain, 24–26 September 2008.

* Corresponding author. Tel.: +34 913466622; fax: +34 913466604.

E-mail address: Antonio.mchaparro@ciemat.es (A.M. Chaparro).

the faradaic efficiency of the overall process (reaction (1)). This situation may occur at low overpotentials and in the presence of chloride ions [12]. Faradaic efficiency may further increase through PtCl_4^{2-} disproportionation giving rise also to Pt chemical deposition:



However this reaction is slow at room temperature [13].

One particular characteristic for the preparation of PEMFC electrode by electrodeposition is the use of a microporous carbon substrate, which constitutes itself the upper part of the gas diffusion layer. Porosity gives rise to three-dimensional electrodes where electrochemical reactions take place under different conditions, compared with planar electrodes. Parameters like conductivities of solid phase and electrolyte, diffusivity of species within the porous structure, and internal surface [14,15], influence the potential distribution within the electrode phase and the time response [16–18]. Electrochemical kinetics on porous electrodes may show double Tafel slope under certain conditions [14,19,20]. Another factor is that the electrochemical reactions only occur in regions penetrated by the electrolyte (flooded region), which may be limited when dealing with aqueous electrolytes and hydrophobic electrodes, as it is the case of carbon black used for PEMFC electrode. All these characteristics must be taken into account for electrodeposition processes on porous substrates. Fundamental studies about electrochemical deposition on a porous electrode have dealt mainly with electrodeposition on flow-through electrodes [21,22], and the growth of porous phase on flat substrate [23]. However, a study of the electrodeposition from an electrolyte in front contact with a porous substrate, as it is used in this work, is lacking to our knowledge.

In this work, PEMFC electrodes are prepared by means of the electrodeposition of Pt on carbon cloth substrate. Substrates are first submitted to an activation process, which gives rise to an increase in the hydrophilic character of the carbon black surface. Then electrodeposition of Pt is carried out by potential cycling in H_2PtCl_6 solution. Electrodeposited electrodes with different Pt loads have been used to prepare membrane electrode assemblies (MEA), and tested as cathodes in single PEMFC. Performance of electrodeposited electrodes is analysed from polarization curves, and compared with commercial electrodes.

2. Experimental

Commercial carbon cloth (ELAT E-TEK, LT1200W, PEMEAS) has been used as substrate for Pt electrodeposition. The substrates are first covered with a carbon black layer of 5–10 μm thickness, by airbrushing with a suspension of carbon black (Vulcan XC-72) and 2 wt% ionomer (Nafion^R, Aldrich 5 wt% solution), in isopropanol. The ionomer is applied to give protonic conduction to the active layer, but in sufficiently small concentration to avoid excessive diffusion barrier for PtCl_6^{2-} anions to carbon grains. Substrates of 16 cm^2 area are activated before electrodeposition, as described below. Electrodeposition of Pt is carried out by submitting to potential cycling between 0.05 V and 0.9 V (100 mV s^{-1}), in a solution of 0.001 M H_2PtCl_6 (Aldrich) in 0.5 M H_2SO_4 (Panreac) and 0.2 M H_3BO_3 (Panreac), and under continuous N_2 bubbling. All solutions have been prepared with pure water (18 $\text{M}\Omega\text{ cm}$, Milli-Q, Millipore). A rectangular three electrode electrochemical cell is used for electrodeposition, to which the substrate is attached on one face, pressed with a graphite plate as back-contact, and sealed with silicone gaskets. A microporous platinum electrode is placed on the opposite face as counter electrode, and mercury/mercurous sulphate (0.68 V vs NHE) is used as reference electrode. Potentials are

applied with a potentiostat (Autolab, PGSTAT 30), and given in this work referred to the NHE.

Morphology and composition of the electrodes have been studied with SEM (Hitachi S-4600) and TEM (JEOL 2100F) microscopies. For TEM analysis, a portion of the active layer is taken from the surface of the electrodes and dispersed in a few drops of isopropanol under ultrasonic stirring. A drop of the suspension is deposited on a Cu grid covered with cellulose.

The membrane electrode assemblies were prepared using a commercial anode (ELAT E-TEK LT120EWALTSI, 0.25 $\text{mg}_{\text{Pt}}\text{ cm}^{-2}$, PEMEAS), Nafion 117 membrane (Aldrich, 178 μm thickness), and the electrodeposited electrode as cathode. Single cells were mounted with these MEAs, using graphite plates with serpentine type flow fields as current collectors, gold plated plates with cell terminals, and steel plates with controlled thermal heating as end-plates.

Single cell testing was carried out with a home-made test bench, under control of cell temperature, feeding gases parameters (humidification, flow rate, temperature, backpressure), and current demand. For start-up, cell is fed with fully humidified H_2 (20 ml min^{-1}) and O_2 (20 ml min^{-1}) at atmospheric pressure, and heated stepwise up to 70 °C, under 70 mA cm^{-2} current demand. The single cell is left during 24 h working under these base conditions. After the start-up process, different characterization measurements are carried out, including polarization curves, voltammeteries for determination of active electrode area, and cross-over test. These measurements are alternated during 3–4 days, leaving the cell working under base conditions between measurements. For polarization curves, cell voltage and the internal resistance measured at 1 kHz (Milliohmmeter, 4338B, Agilent) were recorded at different current demands, from upper to lower values, allowing for voltage stabilization (5–15 min) after each step. Normally, curves were obtained at 70 °C cell temperature, under 1.5/3 H_2/O_2 stoichiometric factor, 1 bar_r/1 bar_r backpressure in anode/cathode, and full gas humidification using water saturators at 70 °C upstream the cell.

Electroactive areas of electrodeposited cathodes (A_{Pt}) were measured by the hydrogen under potential deposition (H_{UPD}) method, while passing H_2 in the anode (30 ml min^{-1}) and N_2 (30 ml min^{-1}) in the cathode, and applying a potential cycle (EG&G PARC potentiostat) in the 0.05 V < V < 1 V range at 30 °C. Pt area was obtained from H_{UPD} desorption charge, using 210 $\mu\text{C cm}^{-2}$ equivalence [24].

3. Results

3.1. Electrodeposition process

3.1.1. Substrate activation

Previous to electrodeposition, the substrate is submitted to an activation process to increase the hydrophilic character of carbon black surface. This process may be carried out by methods based on carbon surface etching, chemically or electrochemically, or by application of wetting additives [6]. Surface etching gives rise to the generation of oxygen containing functional groups that increase interaction with water and improve wettability [25]. We have used for activation the electrochemical method, by voltage cycling in 0.5 M H_2SO_4 solution (0.5 V < V < 1.3 V, 100 mV s^{-1}). Blank voltammeteries before and after activation are given in Fig. 1, showing a considerable increase in double layer charging current of the activated electrode, as a consequence of the larger electrochemical contact. The estimated thickness for this layer is 20 μm , calculated from the double layer capacitance at 0.7 V, and taking for carbon black film 240 $\text{m}^2\text{ g}^{-1}$ specific area, 12.6 F g^{-1} specific capacitance [26], and 0.264 g cm^{-3} density.

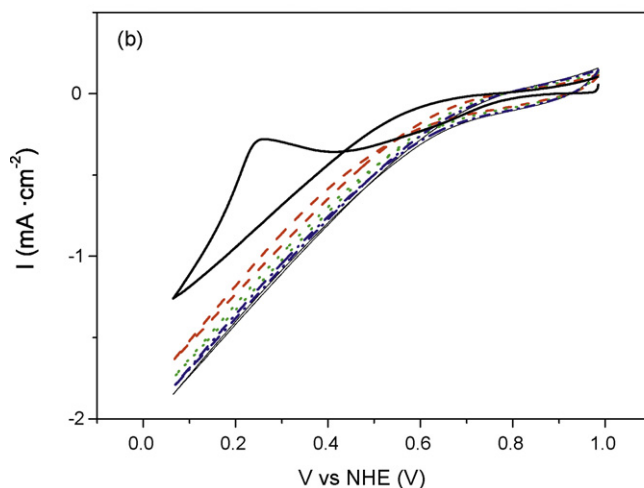
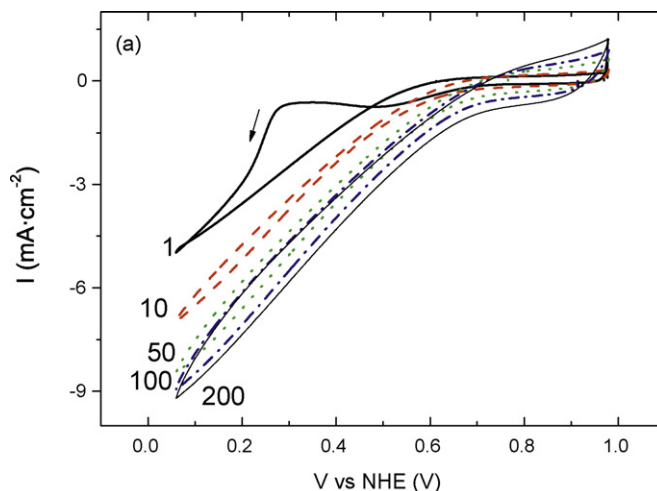
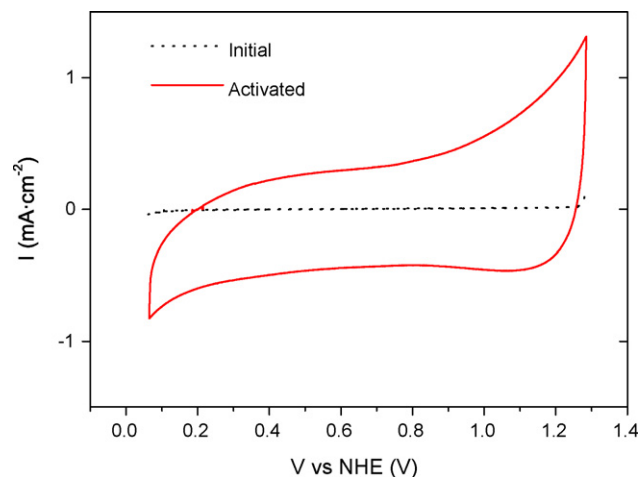


Fig. 2. Cyclic voltammetry on the activated (a) and non-activated (b) carbon black substrate, in 0.001 M H_2PtCl_6 , 0.5 M H_2SO_4 and 0.2 M H_3BO_3 , under continuous N_2 bubbling. Indicated in (a) the cycle number.

to the incomplete electroreduction of PtCl_6^{2-} to PtCl_4^{2-} at potentials close to the thermodynamic value. However, concerning the faradaic efficiency measured during PEMFC electrode preparation, i.e. Pt deposition on the gas diffusion layer, results from Popov and co-workers [6,7], using constant current pulses, reflect lower values, in the range of 10–30%. In our case, the ex situ determination of Pt concentration with ICP spectroscopy carried out on some electrodes have given some higher values, about 50% efficiency,

3.1.2. Electrodeposition voltammetries

Voltammetric curves during platinum electrodeposition are shown in Fig. 2, corresponding to electrodeposition on substrates submitted to activation (a) and non-activated (b). Both cases show significant electrodeposition overpotential during the first cathodic sweep, when nucleation and growth of Pt takes place directly on carbon black surface sites. The same behaviour during first cycle indicates that activation has not changed the electrodeposition kinetics, so the new generated surface functional groups do not seem to work as new nucleation centres, but just to improve interaction with water, and, in general, the hydrophilic character of the carbon black surface layer. During following cycles, electrodeposition overpotential decreases and current increases, due to platinum growth on previously generated platinum centres (secondary nucleation [27]).

The Pt loads of electrodeposited electrodes have been calculated from the electrodeposition charge. Values for five different electrodes are given in Table 1. These values must be considered an upper estimation, since the electrodeposition of Pt from reaction 1 may proceed with variable faradaic efficiency. For instances, efficiency close to 100% has been reported for the electrodeposition of Pt on C, when polarising at 0.1 V [28]. Similar result is observed from a study of Pt deposition on carbon black with the electrochemical quartz crystal microbalance, including a dependence with precursor concentration and deposition potential [29]. Our results on Pt electrodeposition on Au substrate reflect efficiencies in the 80–100% range, with 100% peak at 0.35 V, and little dependence on voltage [30]. A peak in efficiency is expected due to the competing hydrogen adsorption and evolution at less positive potentials, and

Table 1
Characteristics of different electrodes prepared by electrodeposition (1–4) and results of single cell testing: number of sweeps in electrodeposition voltammetry (n), substrate activation, Pt load, Pt roughness coefficient, specific area, Tafel slope (b), exchange current density (i_0), internal resistance measured at 1 kHz ($R(1 \text{ kHz})$), low frequency internal resistance ($R(1f)$), and mass specific currents at 0.8 V and 0.55 V. Data are also given for a commercial electrode (Com).

Ref.	Sweeps no.	Act ^a	Pt load ^b mg cm ⁻²	Rough. ^c	Pt area m ² g _{Pt} ⁻¹	b (mV dec ⁻¹)	i_0 ($\times 10^7$ A cm ⁻²)	R_i (1f) (m Ω cm ²)	R_i (1 kHz) (m Ω cm ²)	$i @$ 0.8 V A g _{Pt} ⁻¹	$i @$ 0.55 V A g _{Pt} ⁻¹
1	200	Yes	0.6	5.6	1.1	67	14	368	304	150	635
2	200	No	0.05	0.77	1.5	86	4.3	384	560	257	3405
3	50	Yes	0.027	0.35	1.3	84	0.2	675	720	23	1123
4	50	No	0.015	0.14	1.0	136	–	–	427	41	1873
Com	–	–	0.25	83	33	69.5	7.4	387	160	309	1384

^a Act: activated substrate.

^b Pt load is determined from electrodeposition charge.

^c Roughness coefficient determined from H_{UPD} area measurements.

that we attribute to the use of the voltage scan procedure. Fixing potentiostatic conditions imposes the interfacial potential to the desired electrochemical reaction, whereas under constant current condition the interfacial potential is a free variable. More complete investigation on efficiency of electrodeposition of Pt for PEMFC electrode preparation is currently being carried out.

3.2. Electrodes characterization

3.2.1. SEM and TEM characterization

The SEM images in Fig. 3 show the substrate surface before (Fig. 3a) and after (Fig. 3b) 200 cycles Pt electrodeposition. It is observed that most substrate particles result fully covered by Pt, at least those on the surface of the electrode. X-ray diffraction and XPS (not shown) confirm the presence of platinum in almost 100% metallic form. Cross section SEM images in Fig. 4 show the profile of Pt distribution for (a) electrodeposited electrode and (b) a commercial electrode (E-TEK, 0.25 mg cm^{-2}). It is observed that the thickness of the active layer, i.e. the layer where Pt electrodeposition has taken place, is restricted to 2–3 μm for electrodeposited electrode compared with 12–13 μm for the commercial electrode.

Characteristics of the Pt phase are better observed on TEM images in Fig. 5. The images are obtained on some active layer particles taken from the surface of an electrodeposited electrode and show that carbon black grains may be partially or totally covered. There is no formation of single particles, but a continuous phase develops with some dendritic morphology towards partially covered particles.

3.2.2. Electroactive area determination

The electroactive area of electrodeposited electrodes was determined by means of underpotential hydrogen deposition charge (H_{UPD}). Fig. 6 shows voltammograms obtained in single cell corresponding to (a) commercial electrode, (b) electrodeposited electrode after substrate activation, and (c) electrodeposited without substrate activation. The activated electrode is characterized by higher double layer charging current due to its higher hydrophilic character. Activation may give rise to oxidative and reductive shoulders at 0.6–0.7 V (Fig. 3b), indicating the presence of a high concentration of oxygen functional groups on the surface of the carbon as a consequence of the activation process [31]. Values of the specific area measured for electrodeposited electrodes on activated substrates are given in Table 1. There is some increase of specific surface on activated electrodes compared with non-activated substrates. However, the largest specific areas are observed on the commercial electrode.

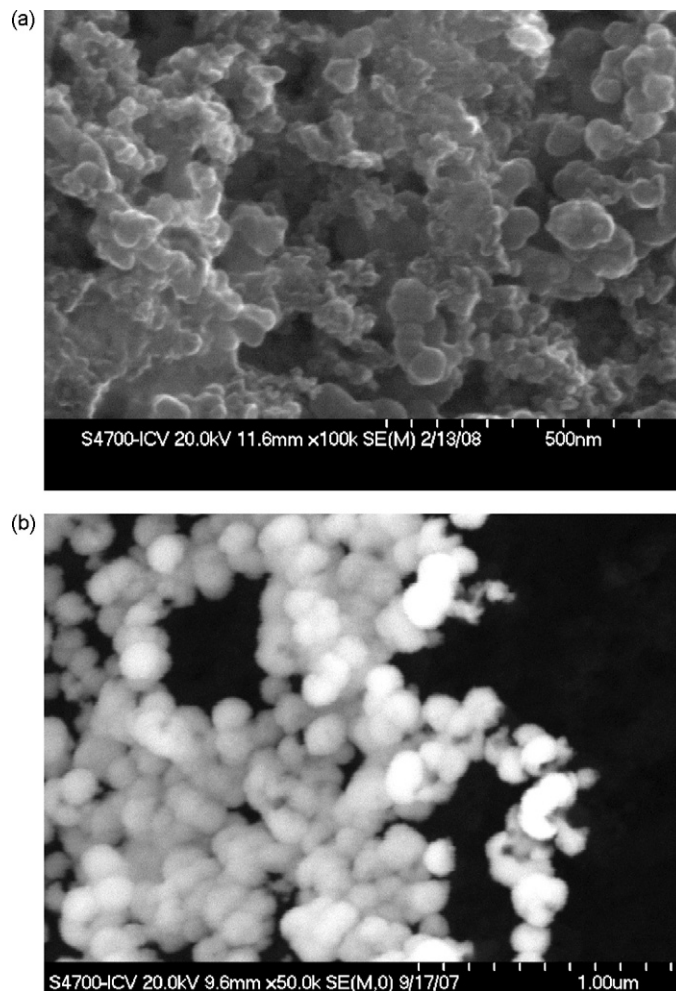


Fig. 3. SEM images of the carbon black surface, before (a) and after (b) electrodeposition of Pt.

3.3. Single cell testing

Single cell testing was carried out after MEA preparation using the electrodeposited electrode as cathode, Nafion^R 117 membrane, and a commercial electrode (0.25 mg cm^{-2}) as anode. For comparison, a reference cell was prepared with the commercial electrode on both anode and cathode sides. Results of polarization curves for electrodeposited electrodes with variable Pt load, as indicated in

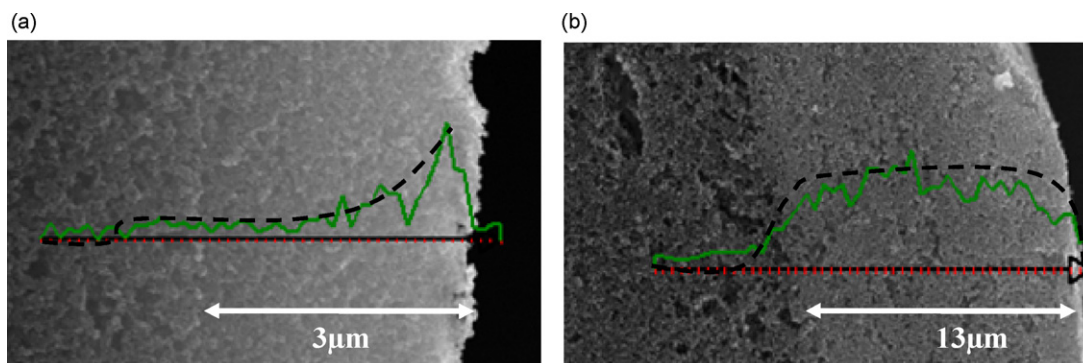


Fig. 4. SEM cross sectional images of the active layer of a Pt electrodeposited electrode (a), and a commercial electrode (E-TEK, $0.25 \text{ mg}_{\text{Pt}} \text{ cm}^{-2}$). Green lines correspond to the Pt concentration profile determined from local EDX analysis. Dashed lines are drawn as visual guide. (For interpretation of the references to colour in this figure legend, the reader is referred to the web version of the article.)

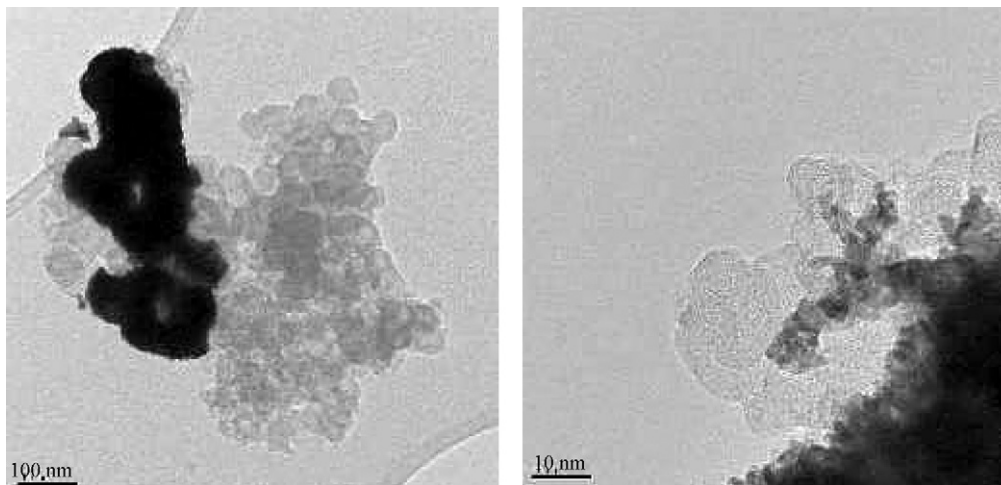


Fig. 5. TEM images of electrodeposited Pt on carbon black.

Table 1, are shown in Fig. 7. Polarization curves were acquired at 70 °C cell temperature, 1 bar_r pressure on both anode and cathode, 1.5/3 constant stoichiometry for H₂/O₂, and full humidification of gases.

Analysis of the curves was carried out by fitting the low current demand range (<100 mA cm⁻²) to the equation:

$$V_{\text{cell}} = E^{\circ} + b \log i_0 - b \log i - iR_i \quad (4)$$

where V_{cell} is the cell voltage, i the cell current density, E° the thermodynamic potential ($E^{\circ} = 1.19 \text{ V @ } 80^{\circ}\text{C}$), b the Tafel slope, i_0 the exchange current density, and R_i the internal resistance. Results of the fitting procedure are given in Table 1. The Tafel slope (b) for a high load electrode shows a value close to the standard (70 mV dec⁻¹). Decreasing Pt load gives rise to higher Tafel slope and lower exchange current density. The values of R_i have been decomposed into two terms:

$$R_i = R_i(1 \text{ kHz}) + R_i(1\text{f}) \quad (5)$$

where $R_i(1 \text{ kHz})$ is the experimentally measured high frequency (1 kHz) resistance, and $R_i(1\text{f})$ is the remaining, low frequency component resistance. It is shown that the electrodeposited electrodes are characterised by higher $R_i(1 \text{ kHz})$ values, which is a parameter related with the resistance of the membrane (Nafion^R 117) and with fast conduction processes inside the electrodes (protonic and electronic conduction). It is probable that this parameter reflects poor electrochemical contact between the membrane and the electrodeposited active layer and/or high resistivity of the active layer.

The specific mass activity is shown in semi-logarithmic plot in Fig. 8. The curves have been calculated from Pt loads determined from faradaic charge (Table 1), hence they give lower limit values of the mass activity of electrodeposited electrodes. Two reference mass activity values, measured at 0.8 V and 0.55 V, are tabulated in Table 1 for comparison. We have taken values at these potentials, instead of 0.9 V as proposed in [32], in order to compare values with lower experimental error. It is shown that the electrodeposited

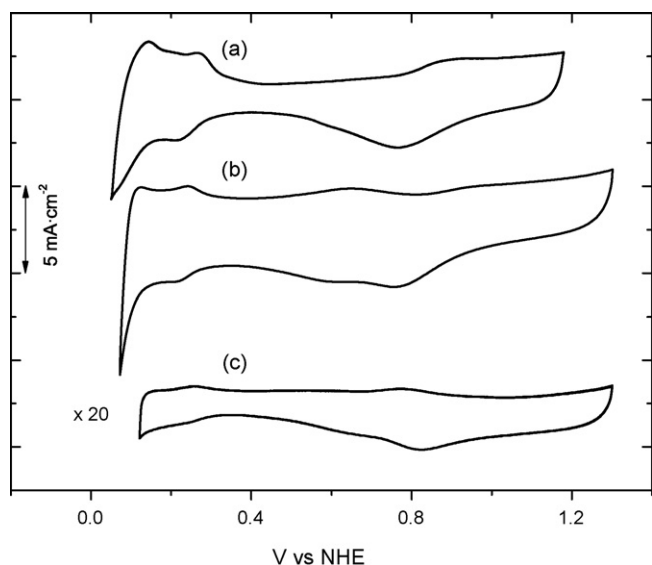


Fig. 6. Single cell voltammeteries on commercial electrode (a), electrodeposited Pt electrode with activation (b) and without activation (c).

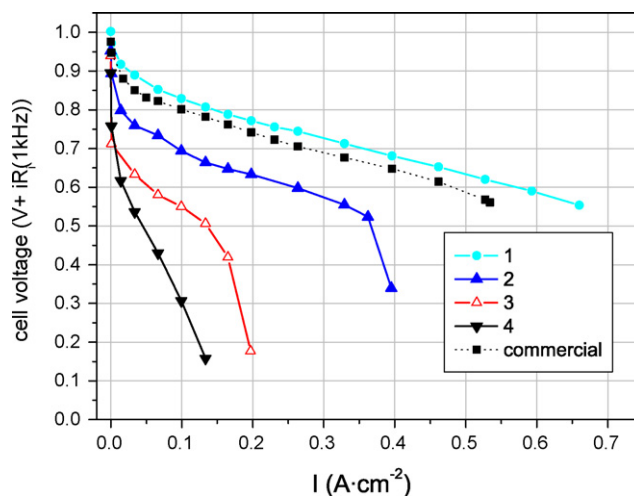


Fig. 7. Polarization curves from single cell testing of MEAs prepared with electrodeposited electrodes as cathode (see Table 1 for electrode characteristics), Nafion 117 membrane and commercial electrode as anode (E-TEK, 0.25 mg_{Pt} cm⁻²). Testing was carried out by feeding anode/cathode with fully humidified H₂/O₂ under 1.5/3 constant stoichiometric ratios, and 1 bar_r/1 bar_r relative pressures. Also shown the curve corresponding to a standard cell.

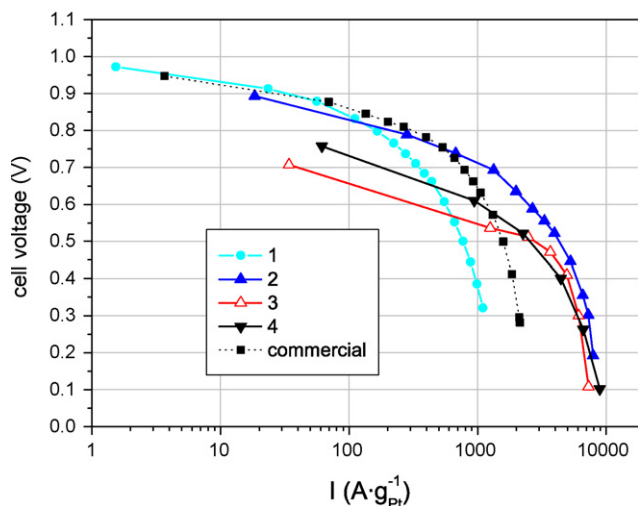


Fig. 8. Mass specific activity from results in Fig. 7.

electrodes with intermediate load (0.05 mg cm^{-2}) have the highest mass activity for cell voltages below 0.75 V .

4. Discussion

4.1. Electrodeposition of platinum on porous carbon black

Given the high porosity of the carbon black substrate, it is of interest to analyse possible influences on the electrodeposition process. According to a one-dimensional model for a porous electrode [16,18], electrode polarization gives rise to a charging current that travels through the flooded region of the electrode with a time constant (τ), given by:

$$\tau = a \cdot c \cdot l^2 \left(\frac{1}{\kappa} + \frac{1}{\sigma} \right) \quad (6)$$

where a is the interfacial surface area per unit volume ($=9 \times 10^6 \text{ cm}^2 \text{ cm}^{-3}$ for Vulcan XC-72 carbon black), c the capacitance per unit area ($=0.4 \mu\text{F cm}^{-2}$), l the thickness of the flooded area (cm), κ and σ the ionomer ($=0.23 \text{ S cm}^{-1}$ for Nafion^R) and carbon phase (43 S cm^{-1}) conductivity, respectively. Eq. (6) predicts a time constant $\tau = 60 \mu\text{s}$ for a $20 \mu\text{m}$ film of carbon black swollen in Nafion^R electrolyte. Therefore, according to this model, homogeneous potentiostatic conditions are established practically instantaneously within the active area (flooded layer) of the carbon black substrate.

Within that porous layer, potentiostatic electrodeposition may be limited either by electrode kinetics or by diffusion of platinum precursor (PtCl_6^{2-}). It was shown in Fig. 2 that electrodeposition is mostly under kinetic control during the first cathodic scan, when generation of first nucleation centres takes place. For the rest of cycles, the overpotential for deposition decreases and current increases, giving rise to a change to diffusion limitation by PtCl_6^{2-} inside the porous carbon-ionomer structure phase. As a consequence, a decay profile of Pt results towards the interior of the flooded area (Fig. 4).

4.2. Performance of electrodeposited electrodes as cathode in single PEMFC

Single cell testing results presented in this work show the performance of electrodeposited electrodes with respect to two main parameters: substrate activation and Pt load (Figs. 7 and 8, and Table 1). Substrate activation allows for higher Pt loading, due to

the increase electrochemical contact area (Fig. 1). The response reflected by polarization curves improves accordingly for electrodes prepared on activated substrates, showing a decrease in Tafel slope (b) and increase in exchange current density (i_0) with Pt load.

On the other hand, the analysis is different when mass specific activities are compared. It must be taken into account that low limit values are presented in Fig. 8 for electrodeposited electrodes. The results show that electrodeposited electrodes may have very high mass activities, which is in accordance with previous works [8], and has been attributed to the allocation of Pt exclusively on areas with electrochemical contact. Mass activity decreases on electrodeposited electrode with substrate activation, as inferred from results in Fig. 8 and Table 1. It appears that activation, although allows for more intense electrodeposition, however the excess Pt does not maintain high mass activity because it is covering previously deposited platinum (cf. Fig. 2). There is an optimum Pt load which, for conditions used in this work, is in the range of $0.05 \text{ mgPt cm}^{-2}$. It may also be possible that activation deteriorates some properties of black carbon support due to generation of oxygen functional groups, like electronic conductivity. This effect may be responsible for the higher loss of mass activity under high current demand on substrate activated electrodes.

On the other hand, it is to be noticed that high mass activity contrasts with low specific area values measured on electrodeposited electrodes, $1\text{--}2 \text{ m}^2 \text{ gPt}^{-1}$ (upper estimation from electrodeposition faradaic charge) if compared with the standard Pt nanoparticles electrode (Table 1). This result may reflect the higher activity of electrodeposited Pt, because it is fully accessible for electrochemical reaction, although confirmation of measured electroactive areas by other methods should be carried out before extracting conclusions from this result.

5. Conclusion

Electrodes for PEMFC have been prepared by the electrodeposition method. The carbon black substrate is previously submitted to an electrochemical activation process, that gives rise to a surface hydrophilic layer. Electrodeposition is carried out by voltage scan, resulting in covering totally or partially carbon substrate grains with platinum. The cross sectional platinum profile shows decay towards the interior of the hydrophilic layer, reflecting a deposition process limited by diffusion of PtCl_6^{2-} . Single cell testing shows higher mass specific activity on electrodeposited cathodes with low and intermediate Pt load (below $0.05 \text{ mgPt cm}^{-2}$). Electrochemical activation allows for higher Pt loads, however additional the Pt has lower mass activity, and, in addition, properties of the black carbon phase may be deteriorated. It is shown that the electrodeposition method is able to prepare PEMFC electrodes with low Pt load and high mass activity. For the preparation of high Pt load electrodes ($>0.05 \text{ mgPt cm}^{-2}$), parameters concerning substrate activation and electrodeposition must be further optimised.

Acknowledgements

This work is financed by Comunidad de Madrid, program ENERCAM-CM (Ref. S-0505/ENE-304), and by Ministerio de Ciencia e Innovación, project DECATEL (Ref. MAT2007-64210).

References

- [1] P.E. Skinner, *Platinum Metals Rev.* 33 (1989) 102.
- [2] O. Antoine, R. Durand, *Electrochem. Sol.-Stat. Lett.* 4 (2001) A55.
- [3] United States Patent 6277261 B1 (2002).
- [4] M.W. Verbrugge, J. *Electrochem. Soc.* 141 (1994) 46.
- [5] S.D. Thompson, L.R. Jordan, M. Forsyth, *Electrochim. Acta* 46 (2001) 1657.
- [6] H. Kim, N.P. Subramanian, B.N. Popov, J. *Power Sources* 138 (2004) 14.

- [7] S.M. Ayyadurai, Y.-S. Choi, P. Ganesan, S.P. Kumaraguru, B.N. Popov, J. Electrochem. Soc. 157 (2007) B1063.
- [8] E.J. Taylor, E.B. Anderson, N.R.K. Vilambi, J. Electrochem. Soc. 139 (1992) L45.
- [9] M.E. Baumgartner, Ch.J. Raub, Platinum Metals Rev. 33 (1989) 102.
- [10] N.N. Greenwood, A. Earnshaw, Chemistry of the Elements, 2nd edition, Elsevier Science Ltd., Burlington, MA, 2002.
- [11] A.T. Hubbard, F.C. Anson, Anal. Chem. 38 (1966) 1887.
- [12] A.L.Y. Lau, A.T. Hubbard, J. Electroanal. Chem. Interfacial Electrochem. 24 (1970) 237.
- [13] A.M. Feltham, M. Spiro, Chem. Rev. 71 (1971) 71.
- [14] R. de Levie, in: P. Delahay (Ed.), Advances in Electrochemistry and Electrochemical Engineering, 6, John Wiley & Sons, New York, 1967.
- [15] J. Newman, C. Tobias, J. Electrochem. Soc. 109 (1962) 1183.
- [16] F.A. Posey, T. Morozumi, J. Electrochem. Soc. 113 (1966) 176.
- [17] S. Devan, V.R. Subramanian, R.E. White, J. Electrochem. Soc. 152 (2005) A947–A955.
- [18] R. Reddy, R.G. Reddy, Electrochim. Acta 53 (2007) 575.
- [19] B.V. Tilak, S. Venkatesh, S.K. Rangarajan, J. Electrochem. Soc. 136 (1989) 1977.
- [20] F. Jaouen, G. Lindbergh, G. Sundholm, J. Electrochem. Soc. 149 (2002) A437.
- [21] D. Pilone, G.H. Kelsall, J. Electrochem. Soc. 153 (2006) D85.
- [22] A.I. Masliy, N.P. Poddubny, A.Zh. Medvedev, A.F. Zherebilov, J. Electroanal. Chem. 600 (2007) 180.
- [23] W. Tiedemann, J. Newman, J. Electrochem. Soc. 119 (1972) 186.
- [24] R. Woods, in: A.J. Bard (Ed.), Electroanalytical Chemistry, vol. 9, Marcel Dekker, New York, 1976.
- [25] W. Shen, Z. Li, Y. Liu, Recent Patents on Chemical Engineering, 1 (2008) 27.
- [26] O. Barbieri, M. Hahn, A. Herzog, R. Kötz, Carbon 43 (2005) 1303–1310.
- [27] L.M. Plyasova, I.Yu. Molina, A.N. Gavrilov, S.V. Cherepanova, O.V. Cherstiouk, N.A. Rudina, E.R. Savinova, G.A. Tsirlina, Electrochim. Acta 51 (2006) 4477.
- [28] A.M. Feltham, M. Spiro, J. Electroanal. Chem. Interfacial Electrochem. 35 (1972) 181.
- [29] T.L. Knutson, W.H. Smyrl, J. Electrochem. Soc. 154 (2007) B1095–B1099.
- [30] A.J. Martín, A.M. Chaparro, L. Daza, J. Power Sources 169 (2007) 65.
- [31] K.H. Kangasniemi, D.A. Condit, T.D. Jarve, J. Electrochem. Soc. 151 (2004) E125.
- [32] K.C. Neyerlin, W. Gu, J. Jorne, H.A. Gasteiger, J. Electrochem. Soc. 153 (2006) A1955.